MRS: NEW GEOPHYSICAL TECHNIQUE FOR GROUNDWATER (GW) WORK

EXPLORATION 07

Jean Roy, IGP
E-mail : jeanroy_igp@videotron.ca

(1) CONCEPTS & IMPLEMENTATION

GROUNDWATER (GW)

Now and in the foreseeable future, humanity needs for fresh water (drinking, agriculture, ecosystems etc.) is going to be increasingly met by groundwater. UNESCO/BGR assessment of global GW resources is summarized in Figure 1.

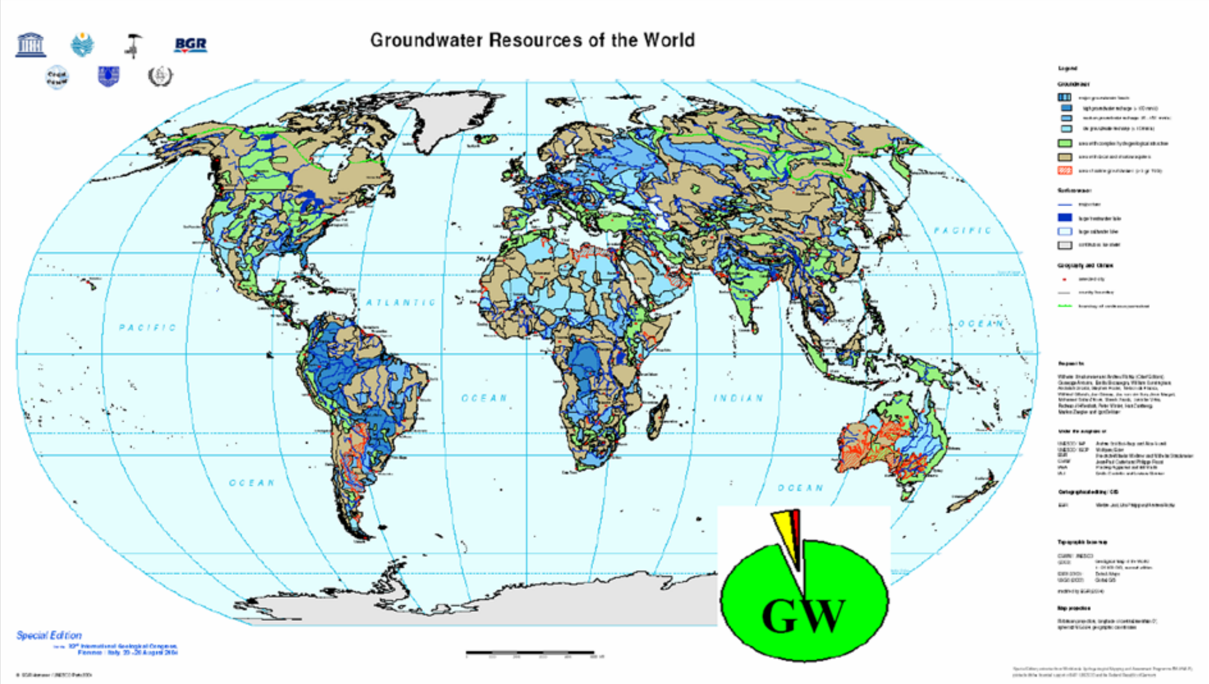

Figure 1: *GW of the world – BGR/UNESCO – pie chart = 'new' water; green sector = GW*

During the last 10 years applied geophysics techniques have made significant progress for the exploration, quantification and management of groundwater. Groundwater (GW) geophysics and hydrogeophysics identify these applications of exploration geophysics. During the last decade, GW geophysics made highly significant progress through the wider applications of the classical techniques and their joint integration (Kirsch, 2006; Rubin and Hubbard 2005; Butler, 2005; Vereecken et al. 2006). Among such classical techniques we have resistivity, induced polarization (IP), spontaneous polarization (SP), time and frequency domain electromagnetics (TDEM, FDEM), ground penetrating radar (GPR), very low frequency EM (VLF), seismic, magnetics, gravity and gamma-ray spectrometry. During that interval, however, one technique stands out as a new and highly relevant geophysical technique for GW: MRS (Magnetic Resonance Sounding).

MRS

Functionally, MRS fits between two known techniques: AAS (Atomic Absorption Spectrometry) and TDEM. AAS is used in laboratories, on carefully prepared samples and has no in-situ depth of penetration but it has good performance for element discrimination and determination of their concentration. TDEM has good depth of penetration, i.e. in suitable cases, it can measure in-situ ground conductivity as a function of depth down to several hundred meters but it has no element discrimination. MRS shares some of these characteristics: it has excellent element selectivity but for 1 element only: hydrogen, a major component of the water molecule. Also, MRS allows moderate depth of penetration in particular over resistive terrain i.e. up to 150 m while quantifying water content and pore-size as a function of depth. MRS is a field application of NMR (Nuclear Magnetic Resonance) to groundwater investigations.

NMR IN A NUTSHELL

NMR (Slichter, 1996) is one of the numerous processes of interaction between electromagnetic (EM) fields and matter. Most of the ones we are familiar with are occurring at the level of electrons, while NMR is a process at the nuclei level. NMR exploits two nucleus properties: (1) a net angular momentum ℓ, (2) a net magnetic moment µ. Only ~ 42 isotopes (30 elements involved, see also Figure 2) have both of these properties in exploitable magnitude. The gyromagnetic ratio $\gamma = \mu/\ell$ is an atomic constant that uniquely characterizes each of these isotopes. Here, we are only concerned with hydrogen nuclei ($^1H^+$) with $\gamma = 2.675 \times 10^8$ rad•s^{-1}T^{-1}. At equilibrium, the net magnetic moment of the volume investigated for a given isotope is aligned with the ambient (static) magnetic field B_s. We can put it out of this alignment (1) by momentarily changing B_s or (2) by exciting the volume at the resonance, Larmor, frequency $f_L = \gamma B_s/2\pi$. After excitation, because of their angular momentum, the excited nuclei will not immediately return to their equilibrium orientation but will rather precess around this direction at the frequency f_L during a relaxation time characterized by decay time constant T_d. See analogy with precessing top on Figure 3. A quantum perspective is also useful for several aspects. Two rotations are of particular interest: *precession* of the nuclei around B_s and *nutation* around the excitation field B_{fl}. The various NMR decay time constants (T_1, T_2 and T_2^*) and their significance in petrophysics are reviewed by Dunn et al. (2002). In ground geophysics, we exploit the NMR process both for magnetometers and for MRS. Various tables summarize the application of NMR to non-invasive sub-surface exploration for water. Table 1 recalls the three magnetic field involved in MRS (excluding noise fields). Table 2 is a simplification of the main observed relationships while Table 3 summarizes the distinction between nuclear precession magnetometer and MRS. In borehole geophysics, NMR logging tools provide diagnostic information for petroleum exploration; due to cost factors, NMR logging is not yet generalized for GW projects.

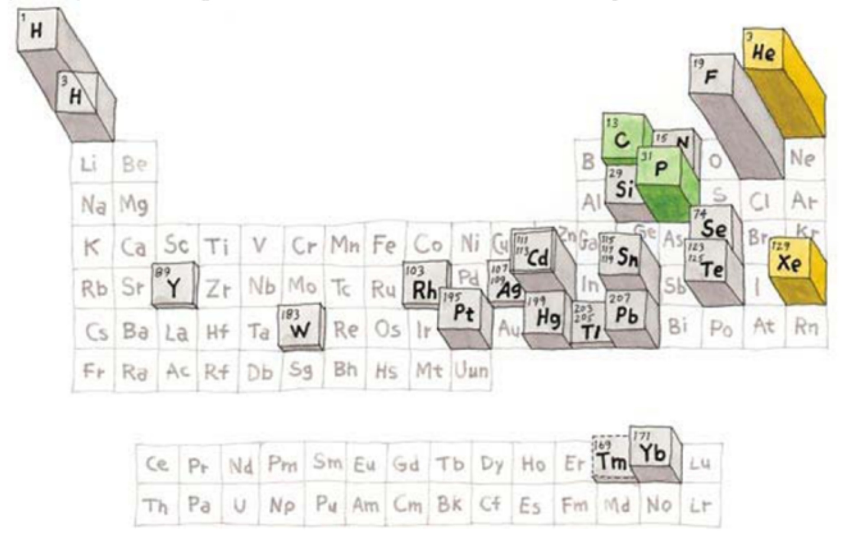

Figure 2: *Some of the isotopes suitable for NMR (Kadlecek, 2002)*

Figure 4: *Hydroscope*

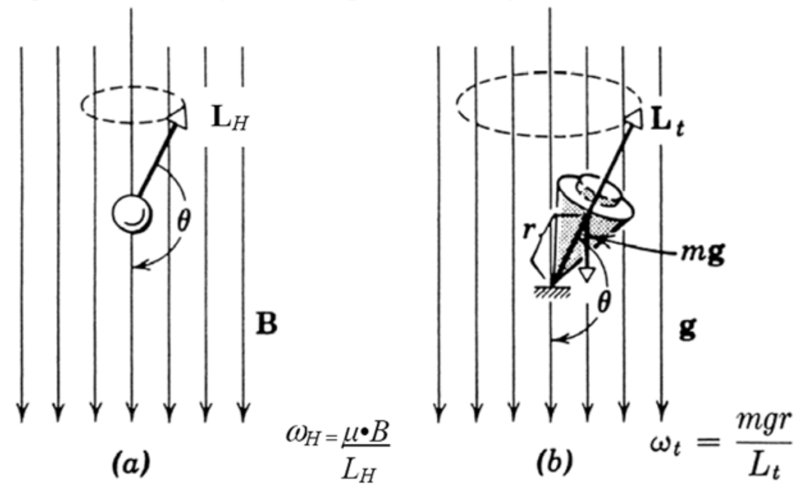

Figure 3: *a) A spinning hydrogen nucleus ($^1H^+$) precessing in the ambient magnetic field: ω_H is the $^1H^+$ precession angular frequency, μ is its magnetic moment ($1.4 \cdot 10^{-26}$ J/T), B is the magnetic field (in T) and L_H is the $^1H^+$ spin angular momentum ($5.3 \cdot 10^{-35}$ J·s). The ratio $\mu/L_H = \gamma$ is called the gyromagnetic ratio. For hydrogen, $\gamma = 2.675 \times 10^8$ rad•s^{-1}T^{-1} b) A spinning top precessing in the ambient gravitational field: ω_t is the top precession angular frequency, mg is its weight, r is the distance between the contact point and the top center of gravity and L_t is the top's angular momentum. In each case the angular frequency is equal to the torque divided by the angular momentum (Halliday & Resnick, 1962).*

Table 1: *The 3 magnetic fields involved in the MRS technique*

Magnetic field	Frequency	Use
Earth's field	DC	Determine f_l e.g.: at 50000 nT, f_l = 2.1 kHz
Excitation field	AC @ f_l	$^1H^+$ resonance excitation
$^1H^+$ field	AC @ f_l	GW [$E_0 \rightarrow \theta_{MRS}$] and pore-size [$T_d \rightarrow$ T] characterization

Table 2: *MRS fundamental equations where* $\boldsymbol{f_l}$ *is Larmor frequency,* $\boldsymbol{\gamma}$ *is the gyromagnetic ratio for* $\boldsymbol{^1H^+}$*,* $\boldsymbol{B_0}$ *is the earth's magnetic field,* **E** *is the NMR signal,* **t** *is the time,* $\boldsymbol{T_d}$ *is the NMR decay time constant,* $\boldsymbol{\varphi}$ *is the phase,* $\boldsymbol{B_\perp}$ *is the component of the excitation field perpendicular to the earth's field,* **r** *is the radius vector,* $\boldsymbol{M_0}$ *is the magnetic moment of the water molecule,* $\boldsymbol{\theta(r)}$ *is the spatial distribution of water content,* **Q** *is the moment of excitation (pulse width times excitation current) and* **v** *is the volume over which the integral is summed.*

Precession (Larmor) frequency, f_l	$f_l = \gamma B_0/2\pi$
Time decay of NMR signal	$E(t) = E_0 \exp(t/T_d) \sin(2\pi f_l t + \varphi)$
NMR signal vs. water content	$E_0 = \int_v 2\pi f_l B_\perp(r) M_0 \theta(r) \sin(\gamma/2 \cdot B_\perp(r) Q)\, dv$

Table 3: *Comparison of the MRS technique with the familiar precession magnetometer, assuming resistive ground and earth's magnetic field =* B_e

	Precession Mag	MRS
Excitation type	DC field >> B_e	AC field << B_e
Excit. field shape	~ uniform	non-uniform
Excit. volume	~ 10^{-4} m^3	up to 10^{+6} m^3
Max Excit. power	~ 10^1 W	~ 10^6 VA (reactive)
What is excited: $^1H^+$	fluid in sensor	in situ GW ≤ 150 m
Time/station	10^{-1} to 10^1 s	~ 10^4 s
What is measured:	signal frequency	signal E_0, T_d, phase
System mass	~ 10 Kg	~ 300 Kg
Info obtained	B_e at sensor's location	θ_{MRS}, T_d depth-wise

MRS IMPLEMENTATION

For MRS work, we use the earth's magnetic field, B_e, as static field i.e. $B_s = B_e$. The practical implementation uses a large loop laid on the ground in a layout quite similar to a single loop time-domain EM set-up (Figure 6 bottom part.). Additional loop shapes are also used see right part of Figure 7. The MRS instrument energizes this loop during the excitation step and uses the same loop as an EM sensor during the detection step. A laptop PC provides control, monitoring, data recording, processing and inversion; it is an essential component of the system. In this implementation (NUMIS^{PLUS}), each module is ≤ 20 Kg (IRIS Instrument, 2001) so that we can do back pack carrying. An earlier implementation, Hydroscope from ICKC (see Figure 4 – to the right of Figure 2) was less portable but allowed to experimentally demonstrate the applicability of the concept.

Figure 5: MRS implementations: top left: original NUMIS, top right: Radic SNMR MIDI, bottom left: NUMIS^{LITE}, bottom right: NUMIS^{PLUS} with EDA magnetometer in monitoring mode at Waalwijk-2.

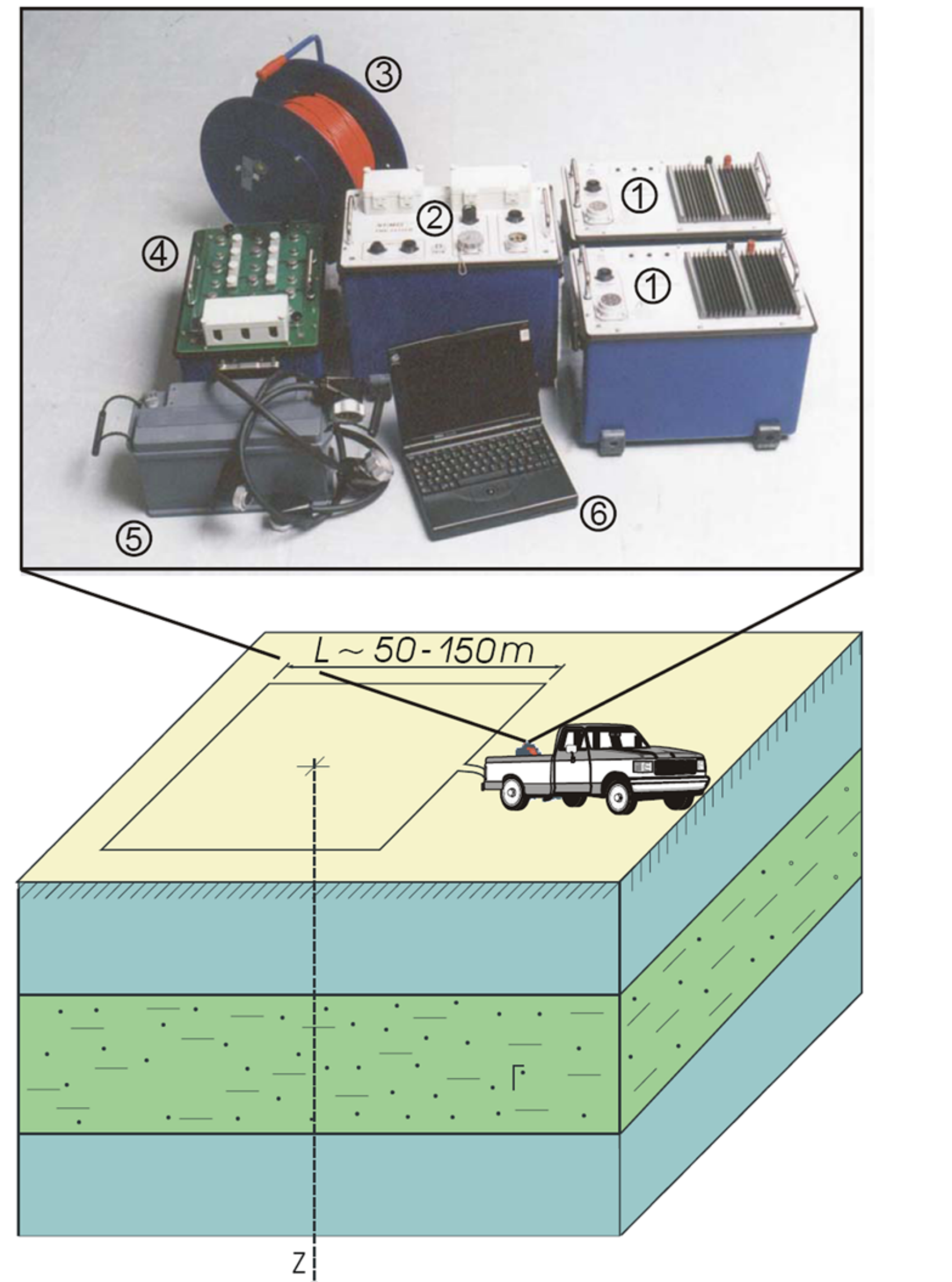

Figure 6: *MRS set-up: - bottom: typical MRS field layout using a square loop; top inset: NUMIS^{PLUS} system - IRIS Instruments (2001): (1): DC/DC converter, (2) main unit, (3) wire loop, (4) tuning box, (5) rechargeable battery, (6) control & data acquisition PC.*

MRS DATA ACQUISITION

MRS data acquisition starts with a magnetic survey to check field homogeneity and determine the local value of f_L. In conductive areas, we add an EM sounding to get the subsurface geoelectrical section at the site. The MRS system is tuned to the local Larmor frequency and a sounding is implemented by varying the 'strength' or pulse moment of the excitation. The pulse moment (Q in A•ms) is the product of loop current times pulse duration. Due to signal to noise ratio (S/N) consideration, each measurement is repeated a number of times for signal stacking purpose in order to improve the S/N. Figure 8 illustrates the summary of such sounding acquired just a few months after Exploration 97 at the margin of a dunes area. The work was done in a park in South-West Netherlands. In this data summary (left panel), three quantities are displayed for each Q value used: the initial value (E_0 - *) of the NMR signal in nV, the average noise level (•) and the signal decay time constant (T_2^* - □) in ms – using the right Y-axis. The sounding parameter, Q for MRS, is the variable that allows depth discrimination. For example, in a Schlumberger vertical electric sounding, the sounding parameter is the operator-controlled, AB inter-electrode distance.

MRS DATA INVERSION

Prior to data inversion, we generate a model of the subsurface MRS response using the value of B_e and its dip, the geoelectrical section and some of the data acquisition parameters e.g. loop size and shape. Typical descriptions of the underlying MRS numerical model include: Goldman et al. (1994), Weichman et al. (2002). Using such model, the data inversion step allows least square fit of the observed data set to the model, using free water content θ_{MRS} and signal decay rates (e.g. T_2^*) as inverted parameters over discrete depth intervals. Below the water table, θ_{MRS} is an estimate (Φ_{MRS}) of the effective porosity, while the signal decay rate is related to the water bearing pore size. In some cases, a more complex excitation scheme is used e.g. Legtchenko et al. (2003), from which an estimate of T_1 e.g. T_1^* is made. Coming back to Figure 8, the two rightmost panels display the result of such inversion step. The center part shows water content as a function of depth while the right part shows the signal decay time again as a function of depth. On the left panel, the full line passing near the "*" symbol shows inverted model response compared to E_0 measured values. Often, because of mixed grain-size or presence of fine sediment, the transition near the water table is gradual rather than abrupt. At the Waalwijk-1 site (Figure 8), the estimated depth of the water table is ~ 8 m. The data inversion strategy and parameters also contribute to a smooth transition between vadoze zone and saturated formations inversion results.

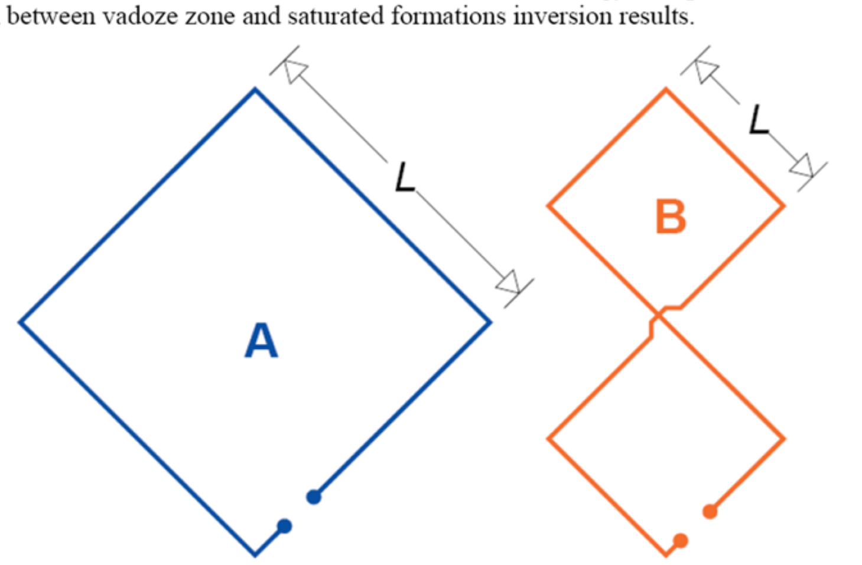

Figure 7: *Two popular loop configuration for MRS: A = 'square', B = 'square-8'*

(2) EXPLOITATION FOR GW INVESTIGATIONS

MRS DATA EXPLOITATION

MRS data acquisition and data inversion typically provide water content and NMR decay time constant as a function of depth. Such empirical data set with its inversion results is displayed at Figure 8 for the case of Waalwijk-1.

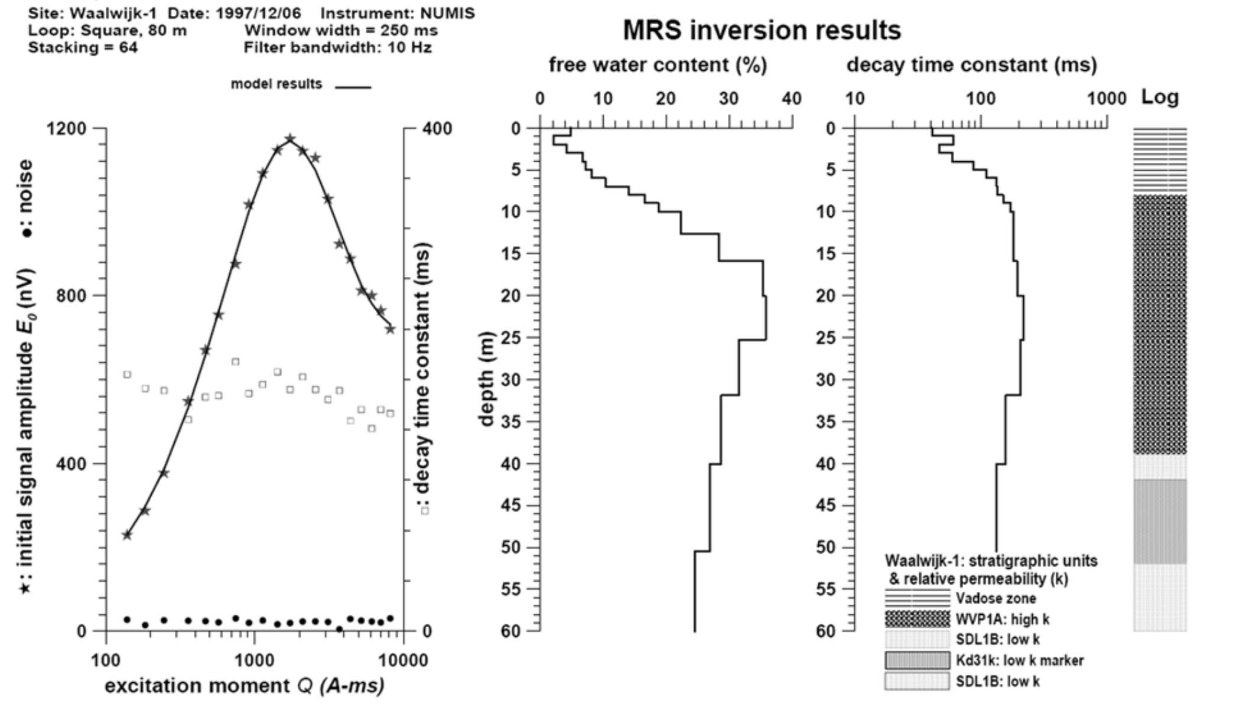

Figure 8: *MRS data set & inversion; Waalwijk-1, Netherlands: from left to right (1) MRS data summary, field [★ - E_0, □ - T_2^*, ● - noise] & model [—] vs. Q, (2 & 3) MRS inversion results: water content & decay time constant vs. depth, (4) Lithological log inferred from three nearest boreholes; in this model, the WVP1A unit has a higher permeability than the SDL1B and Kd31k units. (Item 4, TNO, 1998).*

Information acquired through MRS surveys allows, under suitable conditions, not only detection and positive identification of water bearing layers but also, the determination of their vertical geometry, i.e. depth and thickness, their free water content i.e. the amount of water free to move under realistic hydraulic gradients and an estimate of key parameters such as hydraulic conductivity, *K*, and transmissivity T (Legtchenko et al., 2004). For a given lithology/mineralogy, the longer the NMR decay rate, the coarser the water bearing pore-size below the water table. This important observation was first explained by Korringa et al. (1962) in their "KST" model. Later, Kenyon et al. (1989) showed empirical observations, which confirmed this model. In fact, the relationship between NMR decay rate and pore-size allows, through decay rate spectra analysis, the determination of pore-size distribution. Figure 9 is a pictorial diagram of the in-situ pore-size estimation process by NMR: the smaller the pore, the fastest the relaxation of the precessing $^1H^+$ nuclei through repeated contacts with the solid grain surface. Figure 10, described in the next section, is a reminder that magnetic effect may interfere if the measuring scheme is too simple. Finally Figure 11 is a summary of the classical study by Kenyon et al. (1989) on the empirical demonstration of the direct relationship between pore-size and NMR decay time.

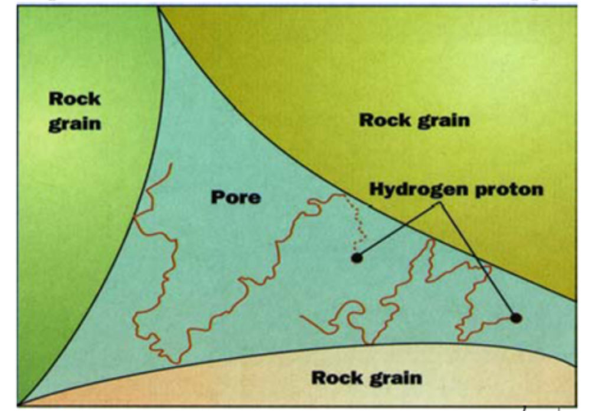

Figure 9: *Schematic representation of $^1H^+$ nuclei free precession within a rock's pore (after Kenyon and Gubelin, 1995)*

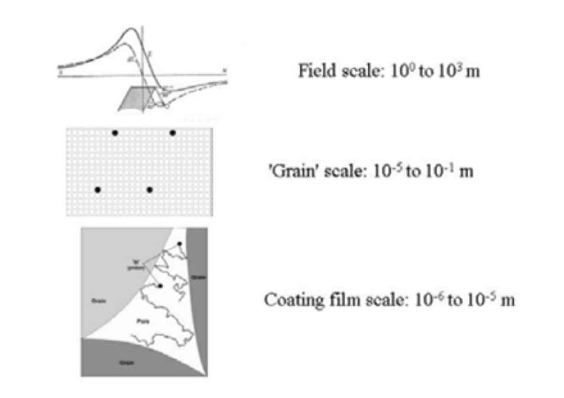

Figure 10: *Magnetic gradients at various scales of concern to MRS*

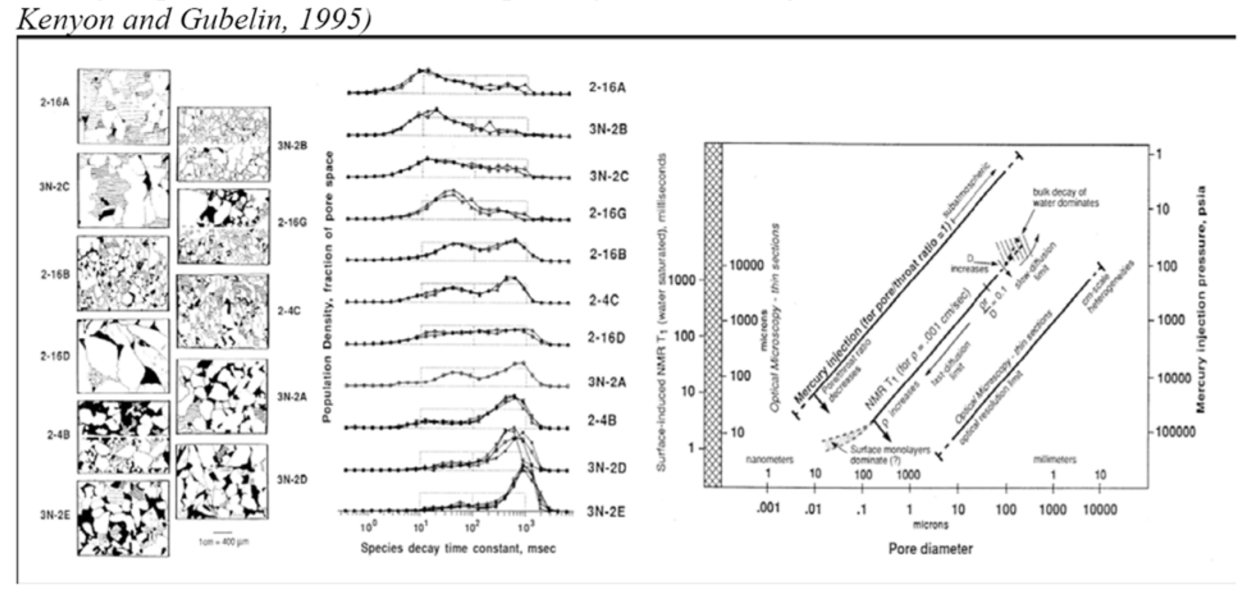

Figure 11: *Pore-size distribution and NMR. Left: micrographs of 11 rock samples; centre: corresponding NMR T1 spectra; right: correlation pore-size vs NMR T1, optical microscopy and mercury injection. The NMR and mercury injection curves are graphically offset for clarity (Kenyon et al. 1989).*

Because of the close link between pore-size, throat size, hydraulic permeability and hydraulic conductivity, NMR logs can reliably supply flow properties information. MRS, which is less advanced than its borehole-logging counterpart, is less reliable in environments where magnetic minerals are present. Also in most cases, MRS supplies an average decay rate instead of a decay rate spectrum. Above the water table, in particular at depths below GPR reach, MRS can supply information difficult to acquire non-invasively, such as water content and water film thickness or water drop size (Roy and Lubczynski, 2005). However, the exploitation of MRS in the vadoze zone still needs calibration. For GW resources assessment, there are four items of main concern: recharge, aquifer storage & flow properties estimation and quality of GW. These are items/tasks are usually done through a combination of techniques including pumping and recovery tests, other hydrogeological methods, numerical model methods including 1D and & distributed models. MRS is most likely to play an increasingly significant role in such resource mapping and quantification strategy.

MRS CAPABILITIES AND LIMITATIONS

Following a little over a decade of tests and evaluations, the users' perspective is that MRS is highly appropriate for GW work due to (1) its inherent selectivity for $^1H^+$ and therefore in the near surface for GW, (2) its performance as a non-invasive sounding tool, i.e. information as a function of depth, (3) the relevance of its inverted parameters to characterize aquifers and aquitards: θ_{MRS} and T_d. MRS is mostly used in a sounding mode, i.e. 1D, and the most readily available information is the one related to water quantity (θ_{MRS}) as a function of depth for both the vadoze and the saturated zone. Its hydrogeological significance needs careful considerations e.g. Lubczynski and Roy (2005). *K* and T calibrations have progressed significantly and lithology dependent factors have already been evaluated e.g. Vouillamoz (2003). An example of the use of signal decay spectral analysis is shown in Figure 12. Such technique is currently limited to MRS data sets with high S/N. In this Figure 3, the water content is resolved into 3 components of pore-size: "fine", "medium" and "coarse". The figure also shows an alternate way of displaying the MRS data set summary: the excitation moment Q is displayed along the Y-axis to stress the relationship (sounding parameter) between Q and depth. On the other hand, the MRS technique is sensitive to ambient noise: MRS cannot be acquired near power lines, industrial installations nor during magnetic storms. The current implementation of the technique is not yet compatible with all geological settings: magnetic materials and some stratigraphic combination of aquifers and conductive layers may generate 'masking' effects e.g. Roy and Lubczynski (2003). Figure 10, schematize sources of magnetic gradient of concern to MRS; magnetic gradients, if not accounted for, can shorten the measured NMR decay rate beyond the MRS instrument aperture window and thus may become insensitive to water in some magnetic rocks. Also some geological structures, e.g. conductive shear zone in an otherwise resistive environment, may channel natural and cultural noise lowering the S/N ratio of the acquired MRS data set.

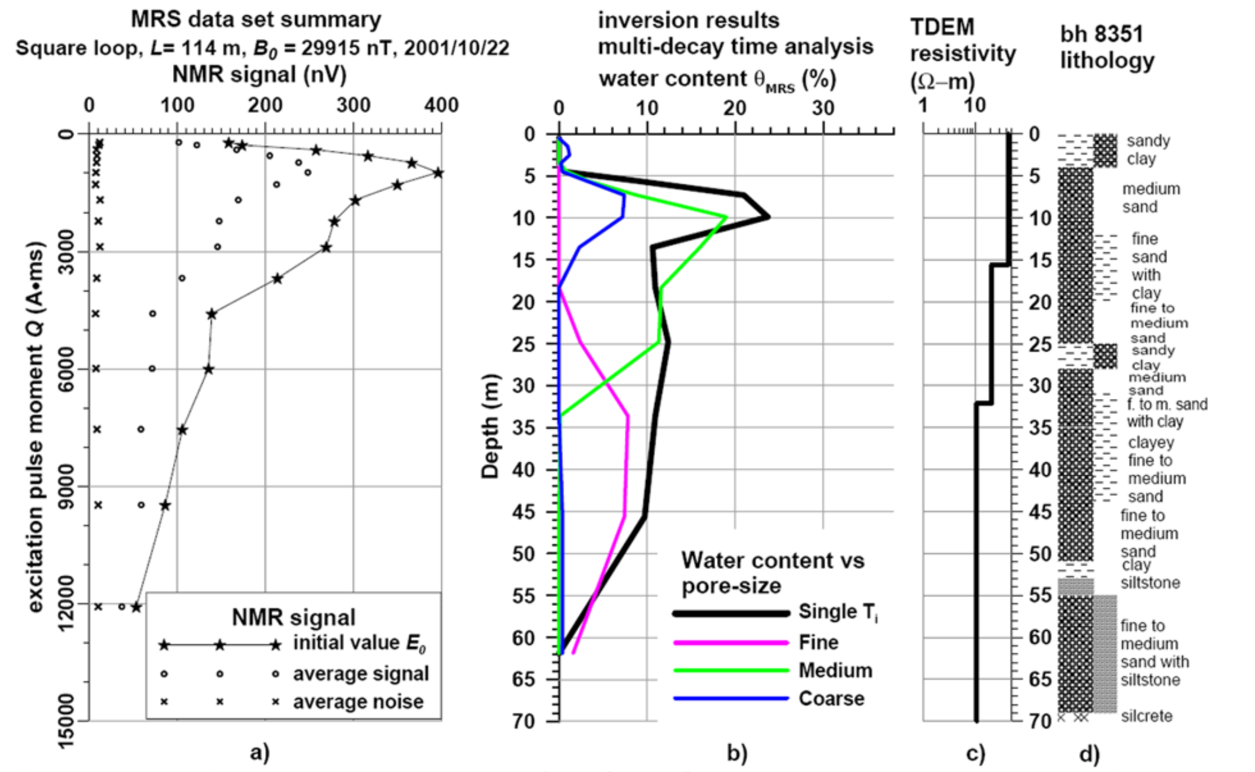

Figure 12: *MRS investigation on a paleo-channel near Maun, Botswana, site BH8351; a) data set summary, b) MRS inversion results with multi-decay time analysis, c) TDEM resistivity, d) BH 8351 lithology (after Mangisi, 2004; Roy and Lubczynski, 2005)*

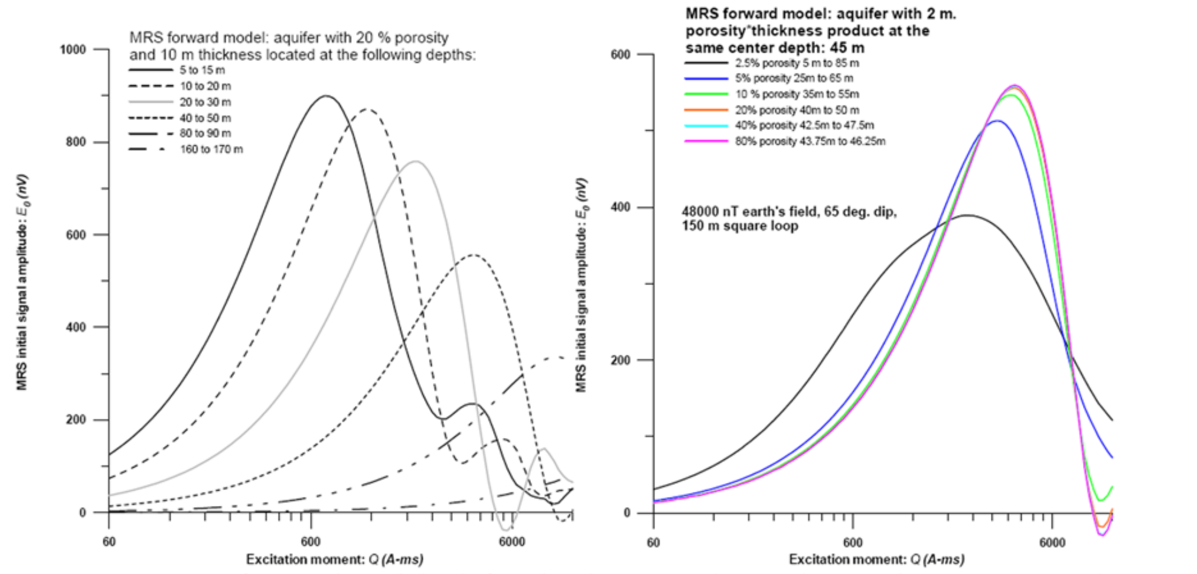

Figure 13: *MRS forward models: left – depth vs. Q relationship; right: MRS equivalence when depth*thickness ≈ or < loop size: L*

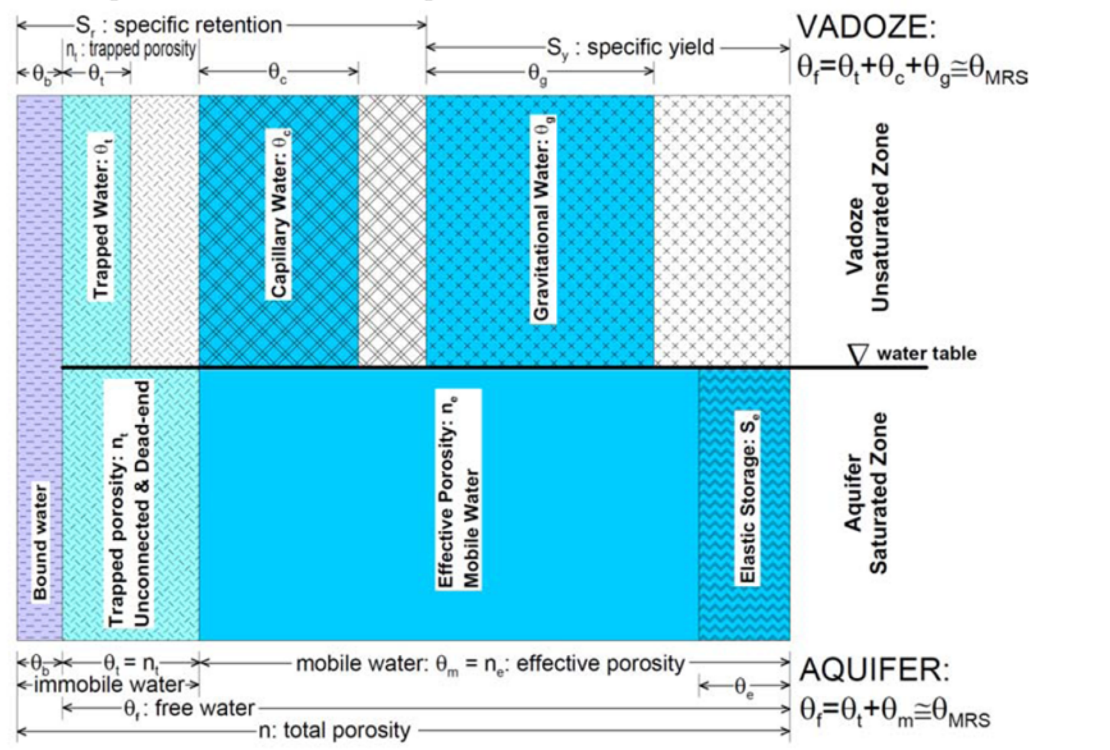

Figure 14: *MRS water content θ_{MRS} and GW storage parameters (after Lubczynski & Roy, 2005)*

Figure 13 illustrates two aspects of the aquifer storage quantification. The left part of the figure clearly shows, through modeling results, the depth discrimination of a 20% porosity 10 m thick aquifer from a mean depth of 10 to 165 m using the excitation moment Q as the sounding parameter. The right part of the figure illustrates a limitation familiar to geophysicists working with electrical techniques: the equivalence limitation. For a porosity*thickness product of 2 m with a mean depth of burial at 45 m, using a 150 m loop size easily resolve an 80 m thick aquifer but will only determine the porosity*thickness product when the thickness is reduced to less than 5 m under the modeled conditions specified in Figure 13. Contrary to most other non-invasive geophysical technique, MRS can discriminate to some extent the kind of water detected. In summary MRS detects mostly free water but Figure 14 goes into much finer details about such discrimination both from the saturated and unsaturated zone. Finally, one of the most difficult discrimination from a geophysical perspective is the separation between the specific yield and the specific retention of the vadoze zone. This is highly dependent on rock grain-size distribution and rock surface properties. Figure 15 is a reminder about empirical observations on that aspect. MRS is not yet calibrated to fully perform such discrimination but progress is ongoing.

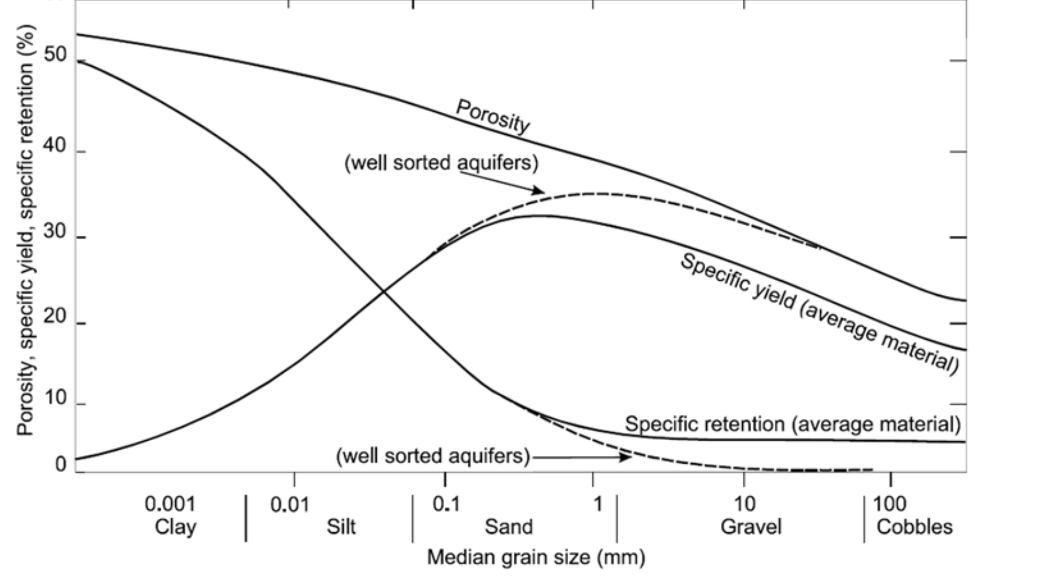

Figure 15: *Relation between specific yield, specific retention and porosity (Stephens et al. 1998)*

MRS ON-GOING R&D

Typical research and development directions involve S/N improvements, 2D & 3D capability and a widening of the NMR signal aperture window. Important progress is made with respect to the hydrogeological control and calibration of the technique. Figure 16 shows transmissivity calibration i.e. pump tests vs. MRS including lithological factors - broadly classified as granites, sands and chalk. After suitable development along several R&D directions, one can expect better ground penetration, higher GW selectivity and higher relevance of inverted parameters than e.g. GPR, possibly with less spatial resolution. However, it is most likely that the optimal use of the MRS technique will be tightly integrated with other geophysical techniques to supply the most relevant information in a rapid and cost-effective way. Currently, the technology is available from France and Russia with other implementations being developed to my knowledge at least in Germany and USA. Active working groups in MRS are located in various parts of the world including in Australia, China, France, Germany, India, Netherlands, Russia, USA etc. Three international workshops have allowed users and designers to share their experience and knowledge on the technique (Berlin 1999, Orléans 2003 and Madrid 2006).

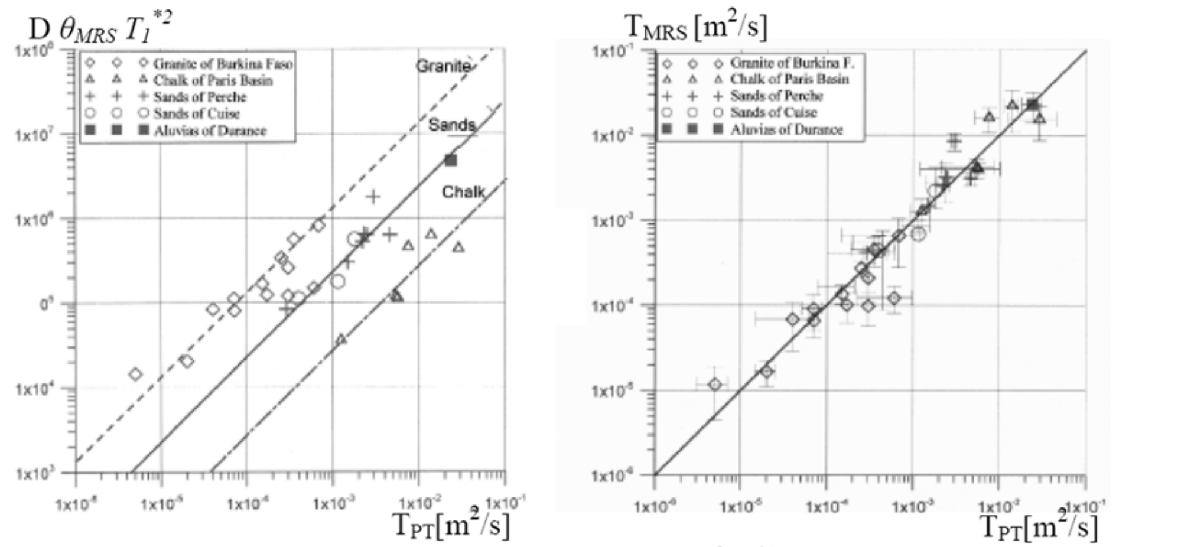

Figure 16: *Comparison: T from pump-tests vs. MRS $\Phi^b T_1^{*2}$ showing lithology -broadly classified as granites, sands and chalk (Vouillamoz, 2003).*

ACKNOWLEDGMENTS

The support of ITC and the collaboration of BRGM, CSIR-Envirotek, DWA-B, DWA-N, Ecole Polytechnique, GSD, GSN, IGM, IRIS Instruments, MBG, UQAC, WCS, WRC are gratefully acknowledged. In particular, I want to acknowledge the 10 years collaboration with my former hydrogeologist colleague at ITC, M. W. Lubczynski.

REFERENCES

Butler, D.W. (ed.), 2005, Near surface geophysics; SEG Investigations in Geophysics series no. 13, 732 p.
Dunn, K.-J., Bergman, D.J. and Latorraca, G.A., 2002, Nuclear Magnetic Resonance Petrophysical and Logging Applications; Pergamon, 293 p.
Goldman M., Rabinovich, B., Rabinovich, M., Gilad, D., Gev, I., Schirov, M., 1994, Applications of the integrated NMR-TDEM method in groundwater exploration in Israel; J. of Applied Geophysics, **31**, 27-52.
IRIS Instruments, 2001, NUMIS^{PLUS}: User's Guide, Data Sheet, System photo; Orléans, France.
Kenyon, W.E., Howard, J.J., Sezginer, A., Straley, C., Matteson, A., Horkowitz, K. and Ehrlich, R., 1989, Pore-size distribution and NMR in microporous cherty sandstones; SPWLA 13th Annual logging Symposium, paper LL.
Kirsch, R., (ed.), 2006, Groundwater geophysics, a tool for hydrogeology; Springer, 493 p.
Korringa, J., Seevers, D.O., and Torrey, H.C., 1962, Theory of spin pumping and relaxation in systems with a low concentration of electron spin resonance centers; The Physical Review, **127**.
Legchenko, A., Baltassat, J. M. and Vouillamoz, J. M. , 2003, A complex geophysical approach to the problem of groundwater investigation; SAGEEP Proceedings, 739-756.
Legtchenko, A., Baltassat, J.-M., Bobachev, A., Martin, C., Robain, H. and Vouillamoz, J.M., 2004, Magnetic Resonance Sounding applied to aquifer characterization; Ground Water, **42**, 363-373.
Lubczynski, M.W. and J. Roy. 2005. MRS contribution to hydrogeological system parametrization; Near Surface Geophysics, **3**: 131-139.
Mangisi, N., 2004, Hydrogeological verification of Magnetic Resonance Soundings, Maun area, Botswana; MSc Thesis, ITC: http://www.itc.nl/library/Papers_2004/msc/wrem/mangisi.pdf
Roy, J. and Lubczynski, M., 2003, The case of an MRS-elusive second aquifer; Proceedings, 2nd MRS Int. Workshop, Orléans, p. 105-108.
Roy, J. and Lubczynski, M., 2005, MRS Multi-exponential decay analysis: aquifer pore-size distribution and vadose zone characterization; Near Surface Geophysics **3**, 4: 287-298.
Rubin, Y. and Hubbard, S.S. (ed.), 2005, Hydrogeophysics; Springer, Water science and technology library, Vol. 50, 523 p.
Slichter, C.P., 1996, Principles of Magnetic Resonance, 3rd ed., Springer-Verlag, 655 p.
Vereecken, H., Binley, A., Cassiani, G., Revil, A. and Titov, K., 2006, Applied hydrogeophysics; Springer, NATO Science Series, Earth and environmental sciences, vol. 71, 383 p.
Vouillamoz, J.M., 2003, La caractérisation des aquifères par une méthode non-invasive: les sondages par résonance magnétique protonique; Thèse de l'Université de Paris XI.
Weichman, P.B., Lun, D.R., Ritzwoller, M.H., and Lavely, E.M., 2002, Study of surface nuclear magnetic resonance inverse problems; Journal of Applied Geophysics **50**, 129-147.